Public Health England

NHS

NHS Breast Screening Programme equipment report

Technical evaluation of Fujifilm AMULET Innovality digital breast tomosynthesis system

February 2018

Public Health England leads the NHS Screening Programmes

About Public Health England

Public Health England exists to protect and improve the nation's health and wellbeing, and reduce health inequalities. We do this through world-leading science, knowledge and intelligence, advocacy, partnerships and the delivery of specialist public health services. We are an executive agency of the Department of Health and Social Care, and a distinct delivery organisation with operational autonomy. We provide government, local government, the NHS, Parliament, industry and the public with evidence-based professional, scientific and delivery expertise and support.

Public Health England, Wellington House, 133-155 Waterloo Road, London SE1 8UG
Tel: 020 7654 8000 www.gov.uk/phe
Twitter: @PHE_uk Facebook: www.facebook.com/PublicHealthEngland

About PHE screening

Screening identifies apparently healthy people who may be at increased risk of a disease or condition, enabling earlier treatment or better informed decisions. National population screening programmes are implemented in the NHS on the advice of the UK National Screening Committee (UK NSC), which makes independent, evidence-based recommendations to ministers in the four UK countries. The Screening Quality Assurance Service ensures programmes are safe and effective by checking that national standards are met. PHE leads the NHS Screening Programmes and hosts the UK NSC secretariat.

www.gov.uk/topic/population-screening-programmes
Twitter: @PHE_Screening Blog: phescreening.blog.gov.uk

Prepared by: CJ Strudley, A Hadjipanteli, JM Oduko, KC Young
For queries relating to this document, please contact: phe.screeninghelpdesk@nhs.net

The image on page 9 is courtesy of Fujifilm.

Published March 2018
PHE publications
gateway number: 2017807

PHE supports the UN
Sustainable Development Goals

Acknowledgements

The authors are grateful to the staff at Burnley Hospital for facilitating the evaluation of the unit at their site.

Contents

Executive summary

The technical performance of the Fujifilm AMULET Innovality digital breast tomosynthesis system was tested in the 2 tomosynthesis modes available, Standard (ST) and High Resolution (HR). The mean glandular dose (MGD) to the standard breast was found to be within the remedial dose levels, except at the high (H) dose setting in HR mode. The threshold gold thicknesses measured with the CDMAM test object are better than the achievable level for 2D, for details of 0.2mm and above.

Technical performance of this equipment was found to be satisfactory, so that the system could proceed to practical evaluation in a screening centre. This report provides baseline measurements of the equipment performance including:

- dose
- contrast detail detection
- contrast-to-noise ratio (CNR)
- reconstruction artefacts, z-resolution
- detector response
- projection modulation transfer function

The MGD and CNR measurements in 2D mode were close to those measured and reported previously.[7]

1. Introduction

1.1 Testing procedures and performance standards for digital mammography

This report is one of a series evaluating commercially available mammography systems on behalf of the NHS Breast Screening Programme (NHSBSP). The testing methods and standards applied are those of the relevant NHSBSP protocols, which are published as NHSBSP Equipment Reports. Report 0604[1] describes the testing of full field digital mammography systems used for 2D imaging and Report 1407[2] describes the testing of digital breast tomosynthesis.

NHSBSP protocols[1,2] are similar to European protocols,[3,4,5] but the European protocols also provide some additional or more detailed tests and standards, some of which are included in this evaluation.

Additional tests were carried out according to the UK recommendations for testing mammography X-ray equipment as described in IPEM Report 89.[6]

1.2 Objectives

The aims of the evaluation were to:

- measure the technical performance of the Fujifilm AMULET Innovality system in tomosynthesis mode
- verify that the dose and noise were as previously reported when the system is operating in 2D mode (Report 1601).[7]

2. Methods

2.1 System tested

Details of the system tested are given in Table 1.

Table 1. System description

Manufacturer	Fujifilm
Model	AMULET Innovality
Target material	Tungsten (W)
Added filtration	50µm Rhodium (Rh) for 2D 700µm Aluminium (Al) for tomosynthesis
Detector type	Amorphous selenium
Detector serial number	J125579
Image pixel size	50µm in 2D images, 100µm in ST and HR reconstructed focal planes, 150µm and 100µm in ST and HR projections
Detector size	240mm x 300mm
Source to detector distance	650mm
Source to table distance	633mm
Automatic exposure control (AEC) modes	AEC, iAEC available in 2D and tomosynthesis modes
AEC dose levels	High (H), Normal (N), Low (L)
Tomosynthesis projections	Fifteen projections without anti-scatter grid equally spaced covering range ±7.5˚ (ST) and ±20˚(HR)
Reconstructed focal planes	Focal planes at 1mm intervals, number equals compressed breast thickness in mm plus 5
Software version	FDR-3000AWS Mainsoft V7.0

The system has 2 tomosynthesis modes:

- Standard (ST) mode which uses a narrow angular range of projections (15°)
- High Resolution (HR) mode which uses a wide angular range of projections (40°)

There is a facility available to carry out a combination exposure, in which a 2D and a tomosynthesis exposure are performed within a single compression.

Fujifilm set up the system for testing in service mode, which has reconstructed tomosynthesis quality control (QC) images available as sets of 2D images corresponding to the individual focal planes, in Digital Imaging and Communications in Medicine (DICOM) CT format. In normal clinical use the reconstructed images would be

available in the standard BTO DICOM format, and this would be a more convenient format for routine QC testing, but should make no difference to the results of these tests. In the CT format images tested the pixel spacing in reconstructed focal planes differs from the image pixel sizes given in Table 1, which are the nominal pixel spacing at the detector. The pixel spacing reduces with increasing height above the detector.

There is a logarithmic relationship between pixel value and detected radiation dose in Fujifilm 2D images and projections. For 2D QC analysis it is necessary to linearize pixel values with respect to dose. To standardise the linearization process the “S” and “L” values used to set the pixel values in the image were set to 121 and 4.0 respectively. In reconstructed tomosynthesis images pixel values have a complex relationship to dose. They are by definition heavily processed and can therefore not be linearized in a manner analogous to the linearization of 2D images. Clinical reconstructed tomosynthesis images from this system are created using the logarithmic projections. For this evaluation Fujifilm also made available reconstructions created using linearized projections, and analysis was carried out using both types of reconstruction to compare their merits for QC purposes.

The reconstructed tomosynthesis images available in QC mode as used for this evaluation excluded some of the image processing applied to clinical images. There are 2 types of post-reconstruction processing available to clinical images: Pattern 1 and Pattern 2. Pattern 2 is less commonly used and therefore the QC reconstructions for this evaluation used Pattern 1.

The system generated a synthetic 2D view (‘S-view’) for each ST and HR tomosynthesis reconstruction, but these were not evaluated

The AMULET Innovality is shown in Figure 1 – image courtesy of Fujifilm.

Figure 1. The Fujifilm AMULET Innovality digital breast tomosynthesis system

2.2 Dose and contrast-to-noise ratio under AEC

2.2.1 Dose measurement

Measurements were made of half value layer (HVL) and tube output across the clinically relevant range of kV and filter combinations. Output measurements were made on the midline at the standard position, 40mm from the chest wall edge of the breast support platform. The compression paddle was in the beam, raised well above the ion chamber. As the system uses different target filter combinations for 2D and tomosynthesis, output measurements were made in both modes. In tomosynthesis mode the stationary exposure option was used.

In both 2D and tomosynthesis modes, exposures of a range of thicknesses of polymethyl methacrylate (PMMA) were made under AEC. For each measurement the height of the paddle was set to match the indicated thickness to the equivalent breast thickness for that thickness of PMMA. In 2D mode exposures were made both with and without the intelligent AEC setting (iAEC) which adjusts exposures according to localised densities in the breast.

MGDs for the standard breast model for 2D and tomosynthesis exposures were calculated using the methods described in the UK and European protocols.[1-5] The

method of measuring MGD in tomosynthesis mode described in the UK protocol differs slightly from the method described by Dance et al [8] in that the incident air kerma is measured with the compression paddle well above, instead of in contact with, the ion chamber. Measurements on other systems [9,10] show that this difference reduces the air kerma and thus the MGD measurement by 3% to 5%.

2.2.2 Contrast-to-noise ratio

For CNR measurements a 10mm x 10mm square of 0.2mm thick aluminium foil was included in the phantom described above, positioned 10mm above the table on the midline, 40mm from the chest wall edge. (The standard position is 60mm from the chest wall edge.)

CNR in 2D mode was assessed using 5mm x 5mm ROIs positioned in the centre of the aluminium square and 2 background positions, to the chest wall and nipple sides of the square, as shown in Figure 2. The CNR in tomosynthesis mode was measured in the focal plane in which the aluminium square was brought into focus. Because the aluminium square was positioned closer than usual to the chest wall edge and there was a gradient in pixel value perpendicular to the chest wall, alternative ROI positions were selected. The ROIs were subdivided into 1mm x 1mm elements and the background ROIs were positioned at the same distance from the chest wall as the aluminium square, as shown in Figure 3. The CNR in tomosynthesis mode was calculated using the average of the mean and standard deviation in pixel values for each 1mm x 1mm element.

CNR was also assessed in the unprocessed tomosynthesis projections acquired for the above images, using a 5mm x 5mm ROI.

Variation of CNR with dose was assessed in the reconstructed focal planes for a simulated breast thickness of 53mm (using a 45mm thickness of PMMA). The variation in central projection CNR with breast thickness and the variation in projection CNR with projection angle for a 53mm thick breast were also assessed.

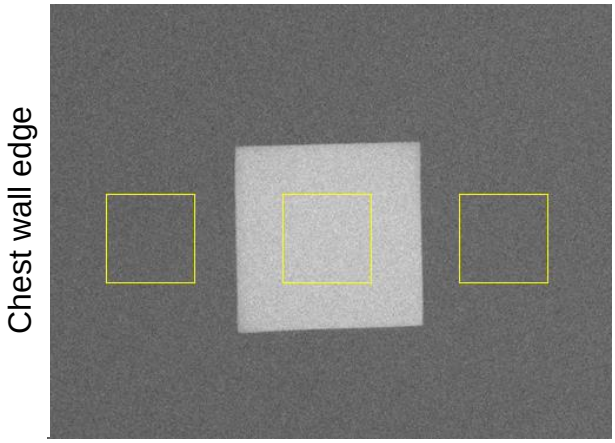

Figure 2. Position of 5mm x 5mm ROIs for assessment of CNR in 2D images

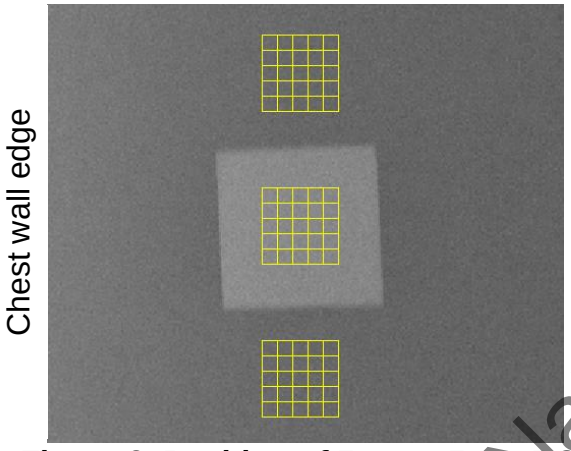

Figure 3. Position of 5mm x 5mm ROIs, subdivided into 1mm x 1mm elements, for assessment of CNR in tomosynthesis focal planes.

2.3 Image quality measurements

Images were acquired of the CDMAM phantom in tomosynthesis mode. The CDMAM phantom (Version 3.4, serial number 1022) was sandwiched between 2 blocks of PMMA, each 20 mm thick. The exposure factors used were manually selected to be as close as possible to those selected by the AEC for an equivalent breast thickness of 60mm. Sets of 8 images were acquired at factors approximating the AEC selected dose level in both ST and HR tomosynthesis modes, and further sets in each mode at 1.5 times the AEC selected dose level.

The focal plane corresponding to the vertical position of the CDMAM within the image was extracted from each reconstructed image. The sets of CDMAM images were read and analysed using 2 software tools: CDCOM version 1.6 (www.euref.org) and CDMAM Analysis version 2.1 (National Co-ordinating Centre for Physics of Mammography (NCCPM), Guildford, UK). This was repeated for the 2 focal planes immediately above and below the expected plane of best focus, to ensure that the threshold gold thickness

quoted corresponded to the best image quality obtained. The fit to the predicted results were used to produce the contrast-detail curves in Section 3.2.

2.4 Geometric distortion and reconstruction artefacts

An assessment was made of the relationship between reconstructed tomosynthesis focal planes and the physical geometry of the volume that they represent. This was done by imaging a geometric test phantom. The phantom consisted of a rectangular array of 1mm diameter aluminium balls at 50mm intervals in the middle of a 5mm thick sheet of PMMA. It was positioned at various heights within a 60mm thick stack of plain sheets of PMMA. The phantom was imaged with the balls at nominal heights of 7.5mm, 32.5mm and 52.5mm above the breast support table. Reconstructed tomosynthesis planes were analysed to yield positional information.

The analysis was automated using a software tool developed at NCCPM (www.nccpm.org). This software is in the form of a plug-in for use in conjunction with ImageJ (http://rsb.info.nih.gov/ij/).

2.4.1 Height of best focus

The height of the focal plane in which each ball was best in focus was identified for each ball. Results were compared for all balls within each image to judge whether there was any variation, indicating possible tilt of the test phantom relative to the reconstructed planes, or any vertical distortion of the focal planes within the image.

2.4.2 Positional accuracy within focal plane

The x (perpendicular to chest wall edge) and y (parallel to chest wall edge) co-ordinates within the image were found for each ball. The mean distances between adjacent balls were calculated using the pixel spacing quoted in the DICOM image header, and compared to the physical separation of balls within the phantom, to assess the scaling accuracy in the x and y directions. The maximum deviations from the mean x and y separations were calculated, to indicate whether there was any discernible distortion of the image within the focal plane.

2.4.3 Appearance of the ball in adjacent focal planes

Changes to the appearance of a ball between focal planes were assessed visually.

To quantify the extent of reconstruction artefacts in focal planes adjacent to those containing the image of the balls, the reconstructed image was treated as though it were a true 3-dimensional volume. The software tool was used to find the z dimension of a

cuboid around each ball which would enclose all pixels with values exceeding 50% of the maximum pixel value. The method used was to re-slice the image vertically and create a composite x-z image using the maximum pixel values from all re-sliced x-z focal planes. A composite z line was then created using the maximum pixel value from each column of the x-z composite plane, and the full width at half maximum (FWHM) in the z direction was found by fitting a polynomial spline. All pixel values were background-subtracted, using the mean pixel value from around the ball in the plane of best focus. This composite z-FWHM (which depends on the size of the ball imaged for the purpose) was used as a measure of the inter-plane resolution, or z-resolution.

2.5 Alignment

The alignment of the X-ray beam to one focal plane of the reconstructed tomosynthesis volume was assessed at the surface of the breast support table, using self-developing film and graduated markers positioned on each edge of the X-ray beam, as indicated by the light field.

The alignment of the imaged volume to the compressed volume was assessed at the top and bottom of the volume. Small high contrast markers were placed on the breast support table and on the underside of the compression paddle, and the image planes were inspected to determine whether all markers were brought into focus within the reconstructed tomosynthesis volume. This was first done with no compression applied and then repeated with the chest wall edge of the paddle supported and 100N compression applied.

2.6 Image uniformity and repeatability

The reproducibility of the tomosynthesis exposures was tested by acquiring a series of five images of a 45mm thick block of PMMA under AEC. A 10mm x 10mm ROI was positioned 60mm from the chest wall edge in a plane 22.5mm above the breast support table, and the mean and standard deviation of the pixel values were found. The signal-to-noise ratio (SNR) was calculated for each image. These images, and others acquired during the course of the evaluation, were evaluated for artefacts by visual inspection.

A combination exposure was carried out using a 60mm thick PMMA test block to test whether the exposure factors matched those for separate 2D and tomosynthesis exposures.

2.7 Detector response

Detector response was measured for the detector operating in tomosynthesis mode. An aluminium filter of 2mm thickness was placed in the beam and attached to the tube port. A typical beam quality (32kV W/Al), was selected and images were acquired using a range of tube load settings in tomosynthesis ST and HR modes. Using a 10mm x 10mm ROI positioned on the midline 50mm from the chest wall edge of the central projection image, the mean pixel value was determined. This was plotted against air kerma incident at the detector.

2.8 Timings

Timings were measured with a stopwatch whilst imaging a 53mm thick equivalent breast, simulated using 45mm PMMA, under AEC, for both ST and HR tomosynthesis modes. Scan times were measured, from when the exposure button was pressed until the compression paddle was released. The time from decompression until the reconstructed tomosynthesis image was displayed on the acquisition workstation was also measured.

2.9 Modulation transfer function (MTF)

MTF measurements were made in tomosynthesis projection images, as described in the European tomosynthesis protocol.[5] This was repeated in ST and HR modes, at heights of 0mm and 40mm above the breast support table, in 2 orthogonal directions (parallel and perpendicular to the chest wall edge).

2.10 Local dense area

The local dense area test was carried out as described in the European tomosynthesis protocol.[5] 40mm PMMA was placed on the breast support table and the compression paddle was positioned at a height of 50mm. Additional small pieces of PMMA (20mm x 40mm) were placed on top of the paddle, on the midline at a distance of 50mm from the chest wall edge, to create additional thicknesses of up to 14mm. For each thickness exposure factors were recorded for the ST and HR tomosynthesis modes under AEC.

3. Results

3.1 Dose and contrast-to-noise ratio under AEC

The measurements of HVL and tube output are summarised in Tables 2 and 3.

Table 2. HVL and tube output measurement in 2D mode

kV	Target/filter	HVL (mm Al)	Output (µGy/mAs at 1m)
25	W/Rh	0.48	9.44
28	W/Rh	0.51	13.1
31	W/Rh	0.54	16.7
34	W/Rh	0.56	20.3

Table 3. HVL and tube output measurement in tomosynthesis mode

kV	Target/filter	HVL (mm Al)	Output (µGy/mAs at 1m)
28	W/Al	0.47	26.4
31	W/Al	0.52	35.3
34	W/Al	0.58	44.6
37	W/Al	0.62	54.2
40	W/Al	0.67	64.1

Calculated MGDs for the standard breast model for AEC exposures in 2D and tomosynthesis ST and HR modes are shown in Figure 4. The remedial dose level used for 2D imaging shown in the figure 4 are from Report 0604.[1] (The reference dose levels in tomosynthesis mode in the European Tomosynthesis Guidelines[5] have the same values as these remedial levels).

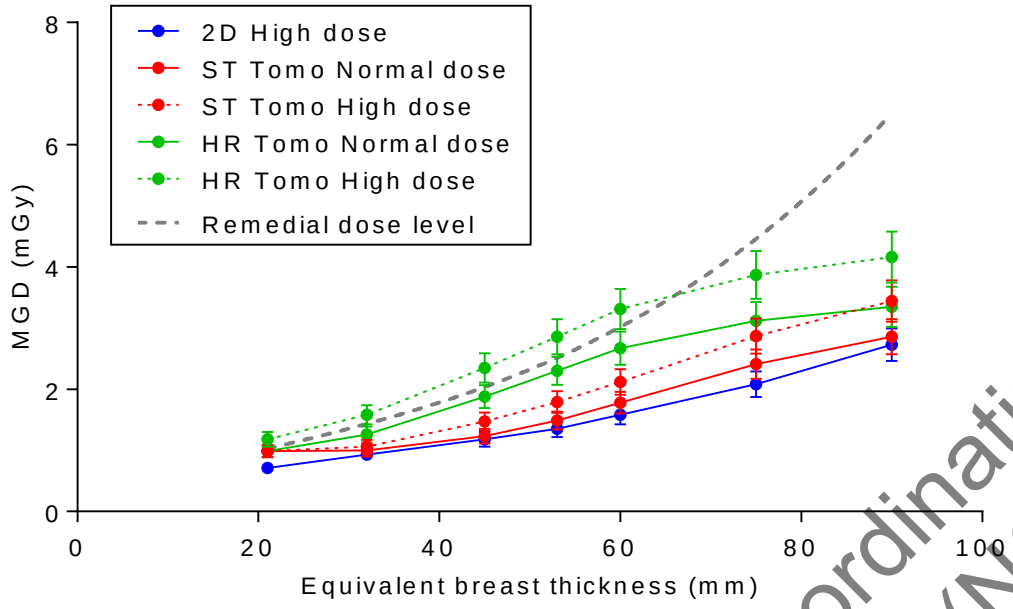

Figure 4. MGD for equivalent breast thicknesses for 2D and tomosynthesis

The CNRs measured in 2D mode for a 0.2mm thickness of aluminium foil are shown for the H dose level in Figure 5.

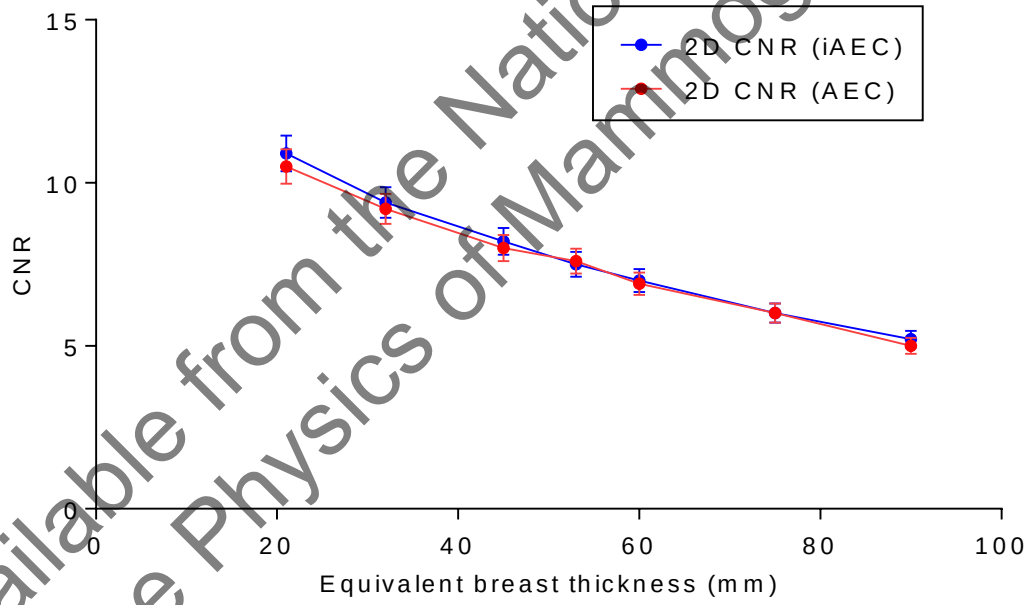

Figure 5. CNR for 2D images obtained under AEC at H dose level

The CNRs measured in reconstructed tomosynthesis focal planes are shown in Figure 6.

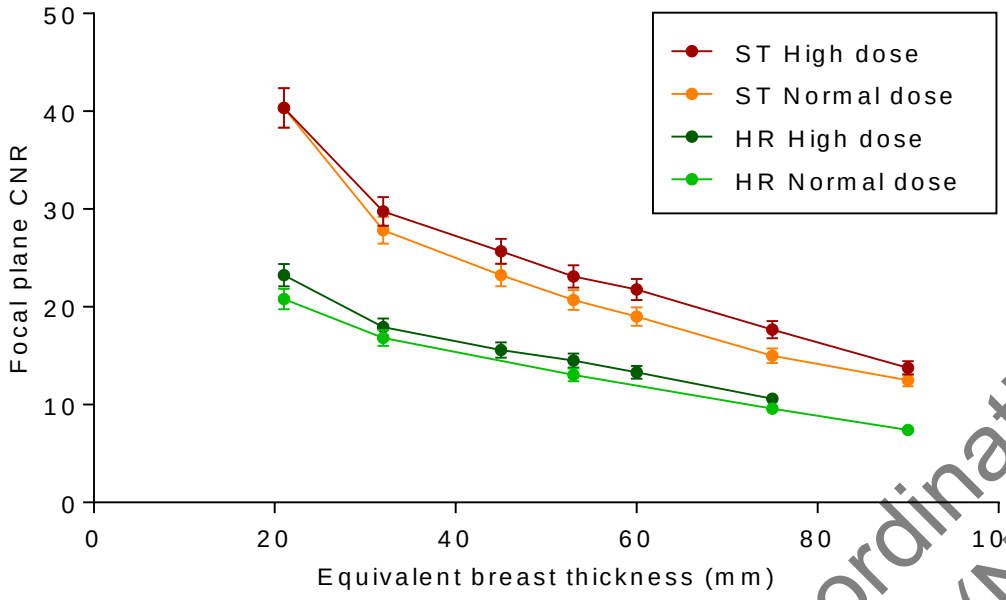

Figure 6. CNR in reconstructed tomosynthesis planes obtained under AEC at the N and H dose levels

The MGD and CNR results shown in Figures 4 to 6 are listed in Tables 4 to 9, together with the exposure factors. All MGDs quoted include the preliminary exposure which is not used in the image.

Table 4. Dose and CNR for 2D images acquired under AEC at the H dose level (AEC mode)

PMMA thickness (mm)	Equivalent breast thickness (mm)	kV	Target/ filter	mAs	MGD (mGy)	Remedial dose level (mGy)	CNR
20	21	26	W / Rh	48.6	0.71	1.0	10.5
30	32	27	W / Rh	71.1	0.93	1.5	9.2
40	45	28	W / Rh	96.2	1.18	2.0	8.0
45	53	29	W / Rh	108.0	1.35	2.5	7.6
50	60	30	W / Rh	122.5	1.58	3.0	6.9
60	75	31	W / Rh	165.7	2.08	4.5	6.0
70	90	33	W / Rh	215.0	2.73	6.5	5.0

Table 5. Dose and CNR for 2D images acquired under AEC at the H dose level (iAEC mode)

PMMA thickness (mm)	Equivalent breast thickness (mm)	kV	Target/ filter	mAs	MGD (mGy)	Remedial dose level (mGy)	CNR
20	21	26	W / Rh	53.1	0.78	1.0	10.9
30	32	27	W / Rh	73.6	0.97	1.5	9.4
40	45	28	W / Rh	101.8	1.25	2.0	8.2
45	53	29	W / Rh	110.6	1.37	2.5	7.5
50	60	30	W / Rh	126.3	1.61	3.0	7.0
60	75	31	W / Rh	171.1	2.10	4.5	6.0
70	90	33	W / Rh	223.7	2.78	6.5	5.2

Table 6. Dose and CNR for ST tomosynthesis images acquired under AEC at the N dose level

PMMA thickness (mm)	Equivalent breast thickness (mm)	kV	Target/ filter	mAs	MGD (mGy)	CNR in focal planes	CNR in central projections
20	21	27	W / Al	32.5	0.99	40.3	7.39
30	32	29	W / Al	30.7	1.00	27.8	5.09
40	45	31	W / Al	35.2	1.23	23.2	4.18
45	53	32	W / Al	41.9	1.49	20.7	3.85
50	60	33	W / Al	46.9	1.78	19.0	3.50
60	75	36	W / Al	52.9	2.41	15.0	2.82
70	90	37	W / Al	65.7	2.86	12.5	2.57

Table 7. Dose and CNR for HR tomosynthesis images acquired under AEC at the N dose level

PMMA thickness (mm)	Equivalent breast thickness (mm)	kV	Target/ filter	mAs	MGD (mGy)	CNR in focal planes	CNR in central projections
20	21	27	W / Al	32.8	0.99	20.8	5.54
30	32	29	W / Al	40.0	1.26	16.8	4.36
40	45	31	W / Al	55.8	1.88	-	3.97
45	53	32	W / Al	66.6	2.30	13.0	3.75
50	60	33	W / Al	72.6	2.67	-	3.40
60	75	35	W / Al	77.8	3.12	9.6	2.62
70	90	37	W / Al	78.9	3.35	7.4	1.98

Table 8. Dose and CNR for ST tomosynthesis images acquired under AEC at the H dose level

PMMA thickness (mm)	Equivalent breast thickness (mm)	kV	Target / filter	mAs	MGD (mGy)	CNR in focal planes	CNR in central projection
20	21	27	W / Al	32.5	0.99	40.3	7.55
30	32	29	W / Al	32.7	1.06	29.8	-
40	45	31	W / Al	42.4	1.47	25.7	-
45	53	32	W / Al	50.5	1.79	23.1	4.33
50	60	33	W / Al	56.2	2.12	21.8	-
60	75	36	W / Al	63.1	2.87	17.7	-
70	90	37	W / Al	79.3	3.44	13.8	2.69

Table 9. Dose and CNR for HR tomosynthesis images acquired under AEC at the H dose level

PMMA thickness (mm)	Equivalent breast thickness (mm)	kV	Target / filter	mAs	MGD (mGy)	CNR in focal planes	CNR in central projection
20	21	27	W / Al	39.4	1.18	23.3	6.14
30	32	29	W / Al	50.3	1.58	17.9	-
40	45	31	W / Al	70.1	2.35	15.6	-
45	53	32	W / Al	83.3	2.86	14.5	4.14
50	60	33	W / Al	90.5	3.31	13.3	-
60	75	35	W / Al	96.8	3.87	10.6	-
70	90	37	W / Al	98.4	4.16		2.25

CNR measurements were also made in the tomosynthesis projection images. Figure 7 shows the variation of CNR with projection angle is shown for ST and HR modes. Figure 8 shows the variation of the central projection CNR with equivalent breast thickness.

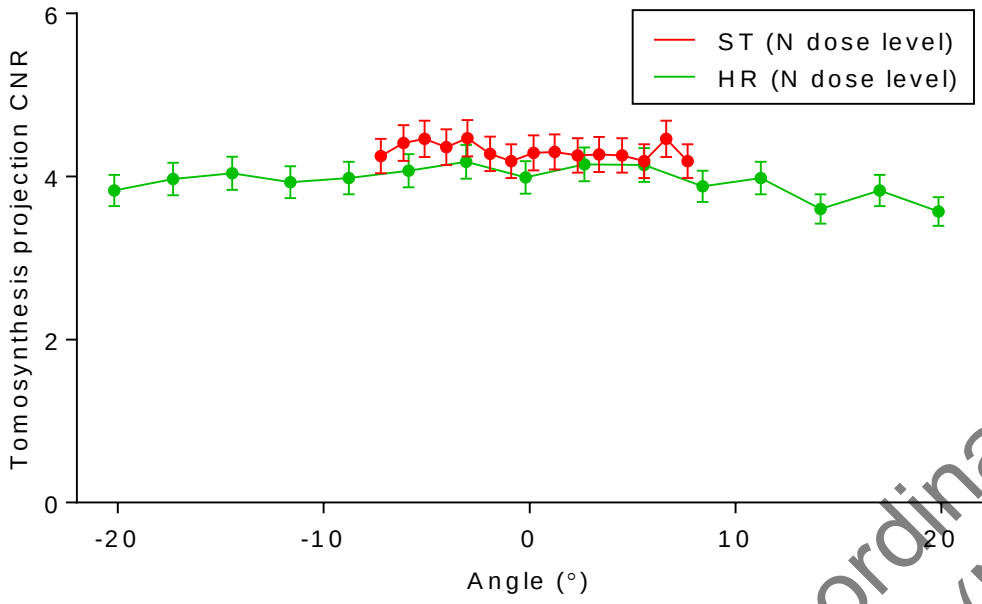

Figure 7. Variation of projection CNR with angle

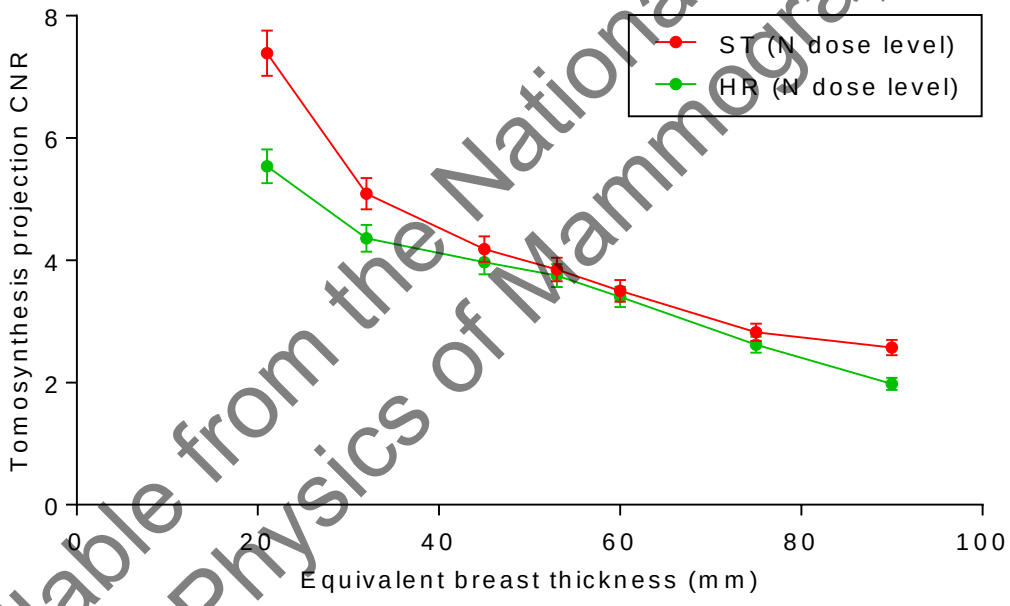

Figure 8. Variation of central projection CNR with equivalent breast thickness

3.2 Image quality measurements

The lowest threshold gold thicknesses were obtained for focal plane 23 in the ST and HR modes. Figure 9 shows the threshold gold thickness detail detection curves for this plane for both modes. In Figures 10 and 11 the threshold gold thickness detail detection

curves are shown for focal plane 23 at the N dose level and at approximately 1.5 times this dose for the ST and HR modes.

The linearized tomosynthesis images were also analysed but the results were not materially different from those presented here.

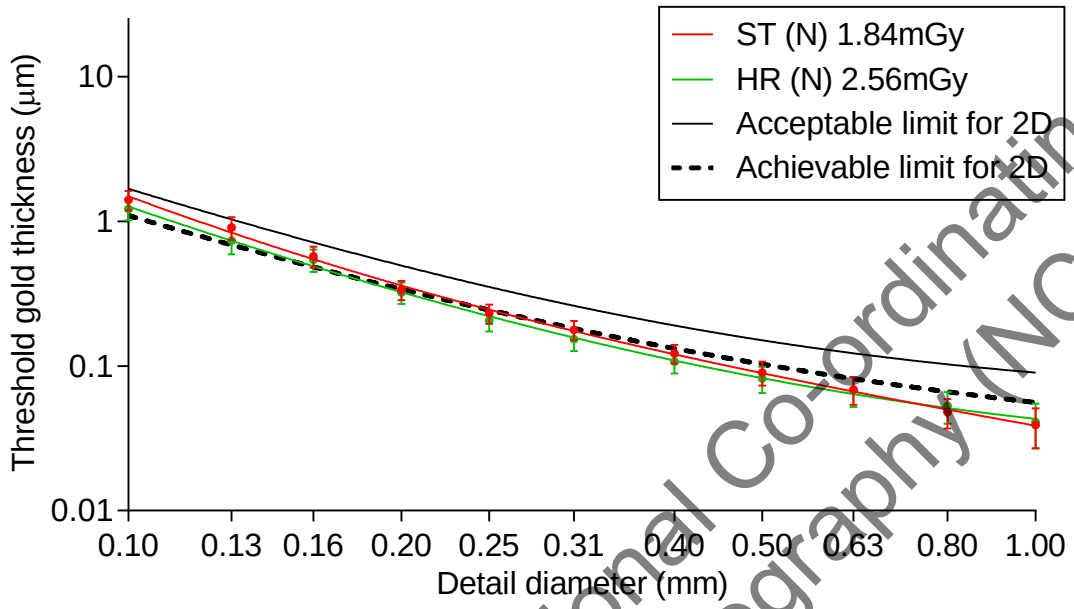

Figure 9. Threshold gold thickness detail detection curves for ST and HR modes for reconstructed focal plane 23, images acquired at AEC N dose level

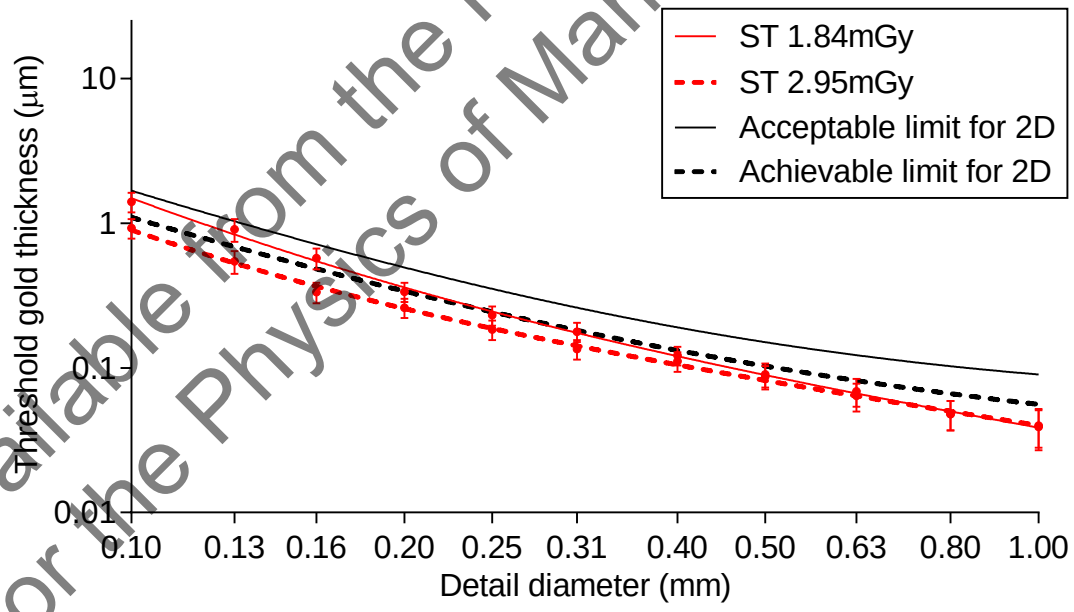

Figure 10. ST mode: Threshold gold thickness detail detection curves for reconstructed focal plane 23, images acquired at 2 dose levels

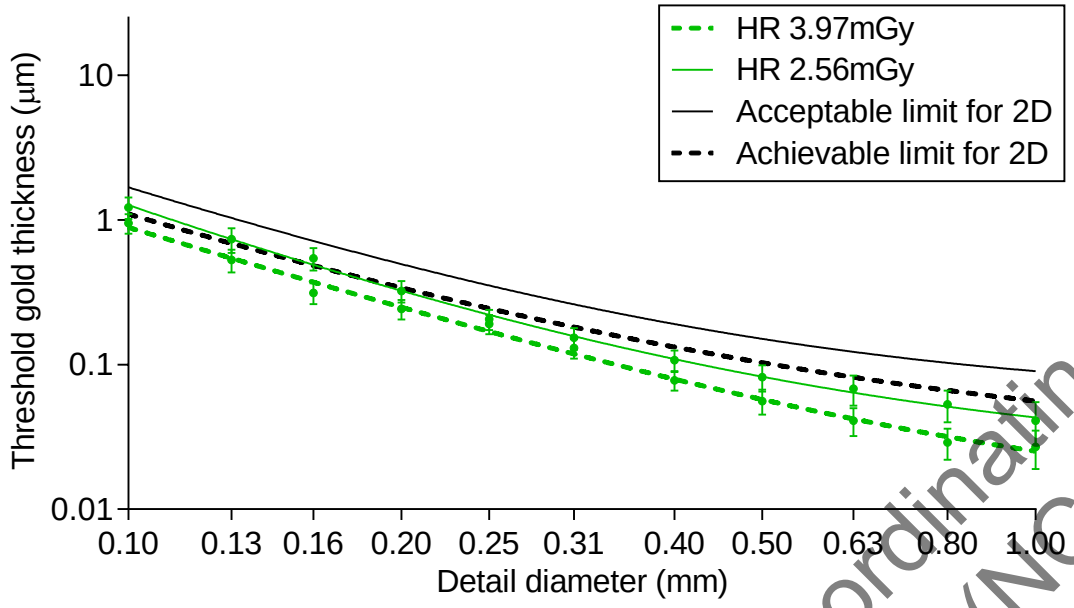

Figure 11. HR mode: Threshold gold thickness detail detection curves for reconstructed focal plane 23, images acquired at 2 dose levels

The threshold gold thicknesses shown in Figures 10 and 11 are summarised in Table 10.

Table 10. Threshold gold thicknesses for reconstructed focal plane 23. The values quoted are the fit to predicted human data calculated as for 2D mammography

	Threshold gold thickness (µm)			
Detail diameter (mm)	ST mode Manual 1.84 mGy	HR mode Manual 2.56 mGy	ST mode Manual 2.95 mGy	HR mode Manual 3.97 mGy
0.1	1.477	1.277	0.901	0.880
0.25	0.245	0.219	0.185	0.169
0.5	0.089	0.083	0.081	0.057
1.0	0.039	0.043	0.041	0.025

3.3 Geometric distortion and resolution between focal planes

3.3.1 Height of best focus

All balls within each image (ST and HR modes) were brought into focus at the same height (± 0.5mm) above the table, and within 1mm of the expected height, with the first focal plane representing the surface of the breast support table. These results indicate that focal planes are flat and parallel to the surface of the breast support table with no

noticeable vertical distortion. The number of reconstructed focal planes is equal to the indicated breast thickness in mm plus 4, indicating that an additional 3 planes are reconstructed above the base of the compression paddle.

3.3.2 Positional accuracy within focal planes

No significant distortion or scaling error was seen within the focal planes. Scaling errors in both the x and y directions, in both ST and HR modes, were found to be less than 0.2%. Maximum deviation from the average distance between the balls was 0.2mm in both modes and x and y directions, compared to the manufacturing tolerance of 0.1mm in the positioning of each ball.

3.3.3 Appearance of the ball in adjacent focal planes

In the plane of best focus the balls appeared well defined and circular. When viewing successive planes, moving away from the plane of best focus, the images of the balls faded and stretched in the direction parallel to the chest wall edge of the image. In ST mode images of the balls persisted more brightly into adjacent planes than in HR mode. The changing appearance of one of the aluminium balls through successive focal planes is shown in Figure 12.

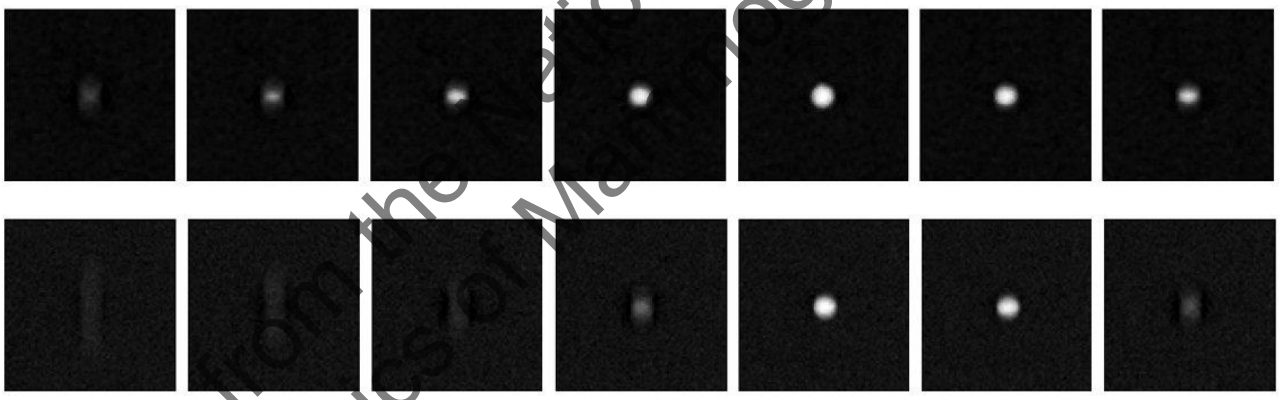

Figure 12. Appearance of 1mm aluminium balls in reconstructed focal planes at 1mm intervals from 4mm below to 2mm above the plane of best focus for ST mode (top row) and HR mode (bottom row)

Using DICOM viewer software it is possible to treat the stack of focal planes as though it were a true 3-dimensional volume and re-slice it vertically to produce planes in the x-z and y-z orientations. The appearance of the ball and associated artefacts in all slices can be visualised in 2 dimensions by creating maximum intensity projections through the re-sliced volumes. Image extracts for a ball positioned in the central area, 120mm from the chest wall, are shown in Figure 13. In these images the z dimension is not to scale relative to the x and y dimensions. Pixels within the focal plane represent dimensions of approximately 0.1mm x 0.1mm, whereas the vertical dimension of each

pixel represents the 1mm spacing of the focal planes. Representation of the x-z and y-z planes using square pixels gives an apparent flattening of the balls, whereas in reality reconstruction artefacts associated with these balls extend vertically by a distance exceeding their diameter.

ST mode:

(i) x-y single plane (ii) x-y all planes (iii) x-z all planes (iv) y-z all planes

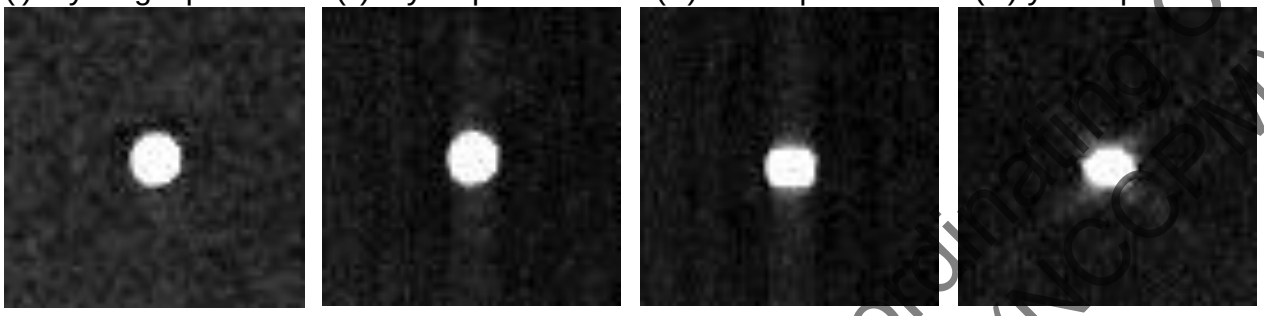

HR mode:

(i) x-y single plane (ii) x-y all planes (iii) x-z all planes (iv) y-z all planes

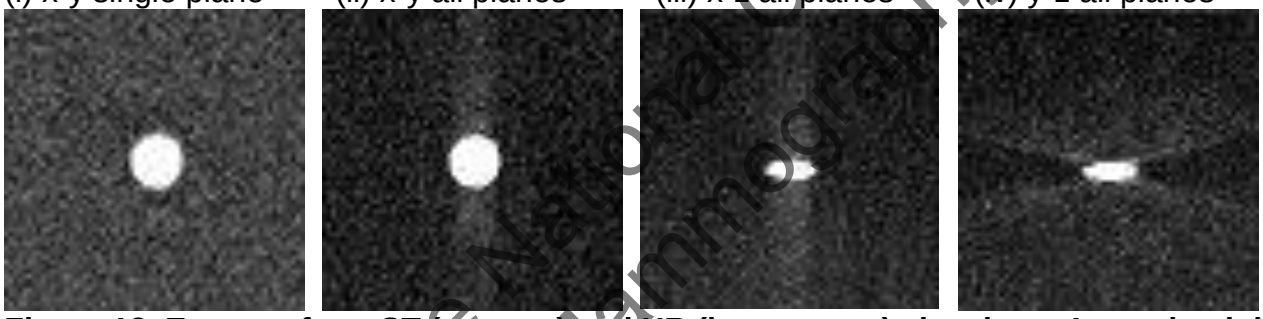

Figure 13. Extracts from ST (top row) and HR (bottom row) showing a 1mm aluminium ball in (i) single focal plane, (ii) the maximum intensity projection through all focal planes, and through re-sliced vertical planes in the directions (iii) parallel and (iv) perpendicular to the chest wall.

Measurements of the z-FWHM of the reconstruction artefact associated with each ball are summarised in Table 10, for images of the balls at heights of 7.5mm, 32.5mm and 52.5mm above the breast support table. The measurements were repeated using the linearized reconstructions produced by the manufacturer, and were found to be similar but approximately 5% greater than the measurements presented in Table 11.

Table 11. z-FWHM measurements of 1mm diameter aluminium balls

	z-FWHM (range) (mm)
ST	7.5 (6.7 to 8.8)
HR	2.8 (2.4 to 4.7)

3.4 Alignment

The alignment of the X-ray field to the focal plane at the surface of the breast support table was assessed. At the chest wall edge the X-ray field overlapped the reconstructed tomosynthesis image by up to 4mm. The lateral edges of the X-ray beam overlapped the edges of the reconstructed image by up to 8mm, therefore remaining well within the boundaries of the breast support table. The X-ray beam overlapped the back edge of the reconstructed tomosynthesis image by approximately 20mm. Alignment was not checked in 2D mode.

Small high contrast objects positioned on the breast support table and attached to the underside of the compression paddle (when no compression was applied) were brought into focus in focal planes approximately 0mm to 2mm from the bottom and 2mm to 5mm from the top of the reconstructed volume. With 100N compression applied and the chest wall edge of the paddle supported, the object at the top of the volume at the centre of the chest wall edge was brought into focus in the top focal plane. (Missed tissue was not assessed at the chest wall edge of the reconstructed image.)

3.5 Image uniformity and repeatability

In both ST and HR tomosynthesis modes the AEC selected the same tube voltage and target filter combination for each of the six repeat exposures and the tubeload varied by less than 1%.

In 2D images, a very faint dark 10mm band was seen along the chest wall edge where the linearised pixel values were reduced by less than 0.5% near the edge. In the ST and HR tomosynthesis images this band at the chest wall was slightly more pronounced and was seen as a pale region of increased pixel value.

A combination exposure (2D and tomosynthesis in the same compression) of 60mm PMMA under AEC resulted in exposure factors within 1% of those obtained for separate exposures.

3.6 Detector response

The detector response for the central projection of ST and HR tomosynthesis images is shown in Figure 14. Also shown for comparison is the detector response for 2D imaging, as measured the evaluation of the Fujifilm AMULET Innovality in 2D mode.[7]

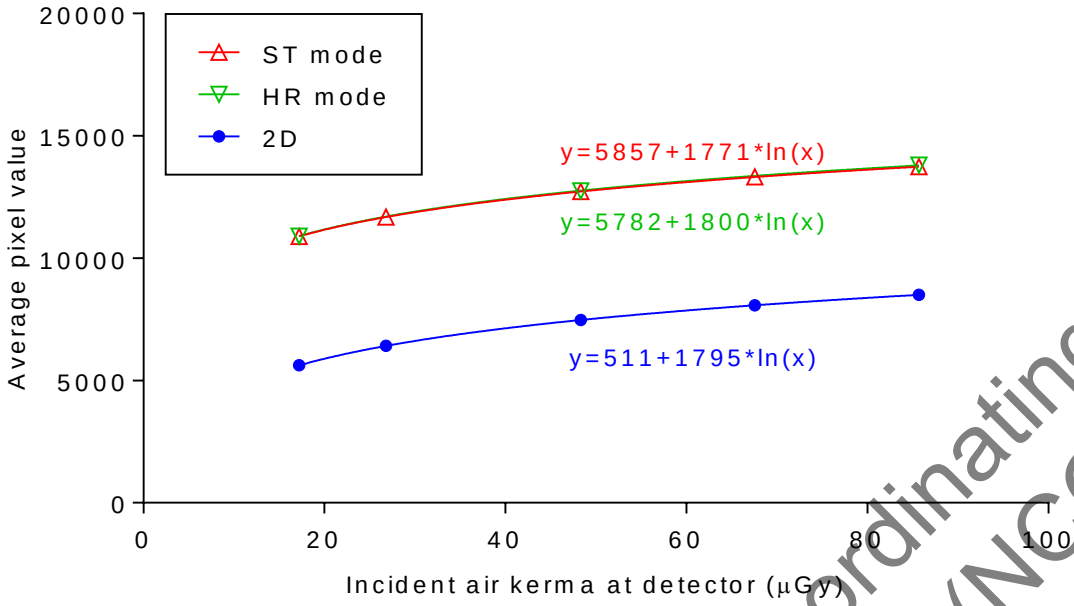

Figure 14. Detector response in 2D and tomosynthesis modes

3.7 Timings

Scan times, and the times from decompression until the reconstructed tomosynthesis view became available, are shown in Table 12.

Table 12. Scan and reconstruction timings

	ST mode	HR mode
Time from start of exposure until decompression	12s	19s
Time from decompression until reconstructed image displayed	18s	26s

3.8 MTF

The MTFs for ST and HR projection images are shown in Figures 15 and 16. Results are shown in the 2 orthogonal directions parallel (u) and perpendicular (v) to the tube axis, at 0mm and 40mm above the surface of the breast support table. These results are summarised in Table 13.

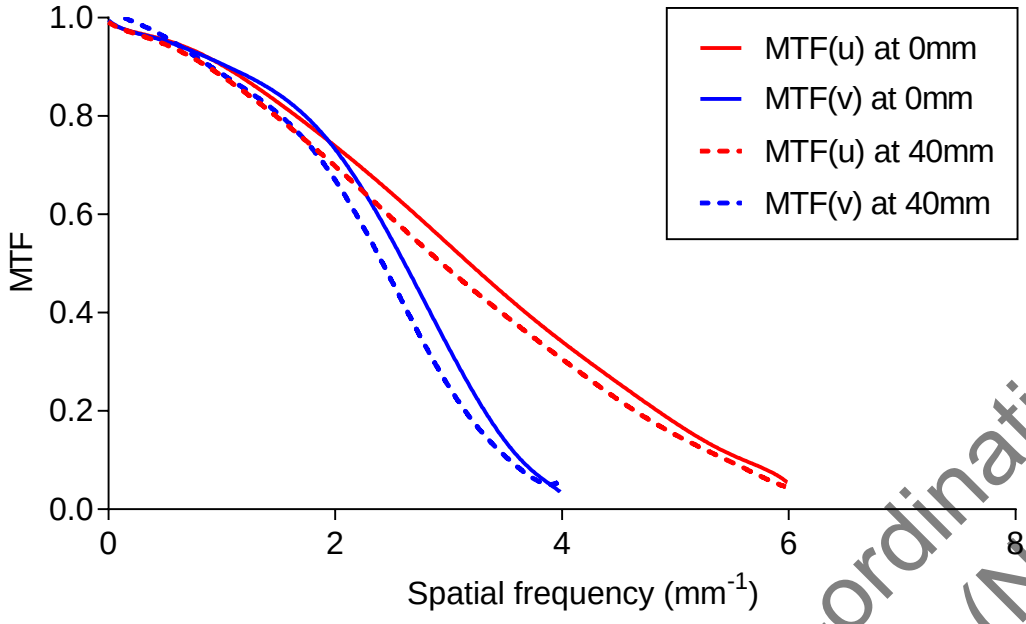

Figure 15. MTF for tomosynthesis projections in ST mode

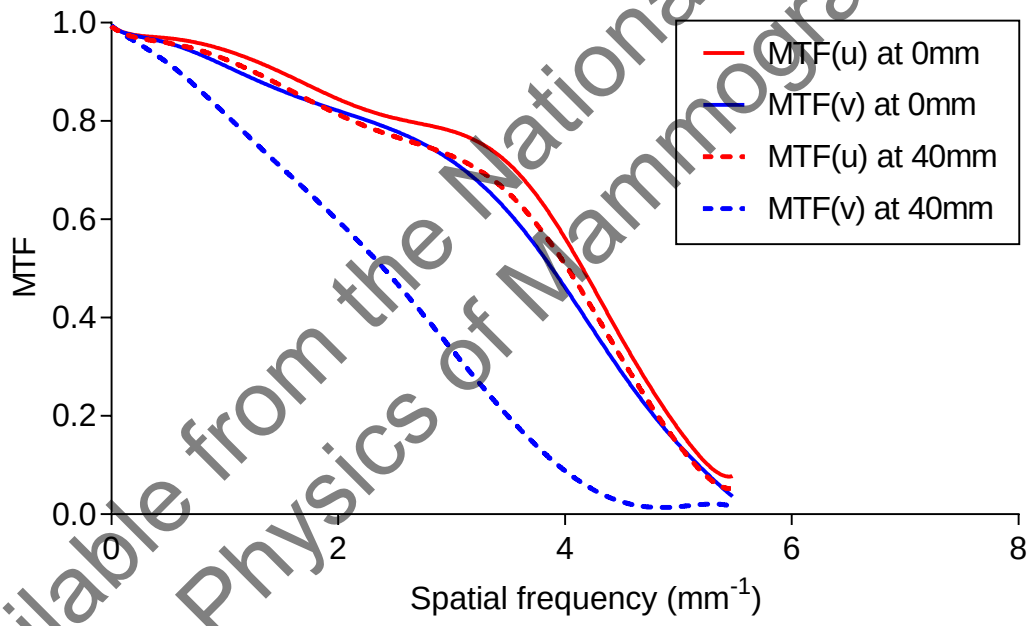

Figure 16. MTF for tomosynthesis projections in HR mode

Table 13. MTF for tomosynthesis projections in the directions parallel (u) and perpendicular (v) to the tube axis

Spatial frequency (mm^{-1})	ST mode				HR mode			
	0mm above table		40mm above table		0mm above table		40mm above table	
	u	v	u	v	u	v	u	v
0.0	1.00	1.00	1.00	1.00	1.00	1.00	1.00	1.00
0.5	0.95	0.95	0.95	0.96	0.97	0.96	0.96	0.92
1.0	0.90	0.91	0.88	0.89	0.94	0.91	0.93	0.81
1.5	0.83	0.84	0.80	0.80	0.90	0.86	0.87	0.71
2.0	0.74	0.73	0.70	0.67	0.84	0.82	0.81	0.60
2.5	0.64	0.55	0.59	0.46	0.81	0.78	0.77	0.47
3.0	0.54	0.33	0.49	0.25	0.78	0.72	0.73	0.34
3.5	0.44	0.14	0.39	0.11	0.71	0.62	0.65	0.20
4.0	0.34	0.03	0.31	0.06	0.56	0.46	0.51	0.09
4.5	0.26		0.22		0.36	0.29	0.32	0.03
5.0	0.18		0.15		0.17	0.14	0.14	0.02
5.5	0.11		0.10		0.08	0.03	0.05	0.01

3.9 Local dense area

Exposure factors in both ST and HR modes were found to remain constant with addition of the small pieces of PMMA, indicating that the AEC does not adjust for local dense areas in tomosynthesis mode.

4. Discussion

4.1 Dose and CNR

MGD and CNR in 2D mode were within about 10% of those measured previously for the Fujifilm AMULET Innovality system.[7] Use of the iAEC option when imaging the CNR test object slightly increased the tube load by up to 10%.

MGDs in the ST tomosynthesis mode at the N and H dose settings and MGDs in the HR tomosynthesis mode at the N dose setting were within the reference dose levels for tomosynthesis systems in European guidance.[5] Doses at the H dose setting in the HR tomosynthesis mode exceeded the reference dose levels for equivalent breast thicknesses up to 60mm.

CNR measurements in ST and HR tomosynthesis images decreased with increasing breast thickness, as is seen in 2D imaging. Increasing the dose at a given breast thickness slightly increased the CNR.

4.2 Image quality

In the absence of any more suitable test object for assessing tomosynthesis imaging performance, the CDMAM test object was used. In ST mode at the N dose level, the threshold gold thicknesses for reconstructed focal planes were better than the minimum acceptable level and, for detail diameters greater than 0.2mm, close to the achievable level of image quality for 2D mammography. The threshold gold thicknesses for HR mode were slightly better than for ST mode. These results take no account of the ability of tomosynthesis to remove the obscuring effects of overlying tissue in a clinical image. The degree of this effect varies between tomosynthesis systems and also differs between the ST and HR modes on this system. Results are quoted for focal plane 23, which in this case gave the best results in each mode. At 1.5 times the AEC selected dose, the threshold gold thickness decreased in both modes, as expected.

A standard test object that would allow a realistic and quantitative comparison of tomosynthesis image quality between systems or between 2D and tomosynthesis modes is not yet available. A suitable test object would need to incorporate simulated breast tissue to show the benefit of removing overlying breast structure in tomosynthesis imaging, as compared to 2D imaging. In the absence of such a test object, clinical trials (real or virtual) are needed to more reliably indicate the clinical usefulness of any tomosynthesis system.

4.3 Geometric distortion and reconstruction artefacts

The reconstructed tomosynthesis focal planes were flat and parallel to the surface of the breast support table. No vertical or in-plane distortion was seen, and there were no significant scaling errors.

The reconstructed tomosynthesis volume was found to start at the surface of the breast support table and continue to 3mm above the nominal height of the compression paddle. This is useful in that it allows for a small margin of error in the calibration of the indicated thickness or some slight tilt of the compression paddle, without missing tissue at the bottom or top of the reconstructed image.

The mean inter-plane resolution (z-FWHM) for the 1mm diameter balls was found to be 7.5mm and 2.8mm, for the ST and HR modes respectively, indicating better resolution in the z-direction in HR mode.

4.4 Alignment

The alignment of the X-ray beam to the reconstructed image was satisfactory.

There was no missed tissue at the bottom or top of reconstructed tomosynthesis images.

4.5 Image uniformity and repeatability

The repeatability of tomosynthesis AEC exposures was satisfactory. A very faint 10mm wide band was seen at the chest wall edges of reconstructed tomosynthesis images.

4.6 Modulation transfer function

In ST mode, more blurring was seen in the direction of tube movement, MTF(v), than in the orthogonal direction, MTF(u). In each direction the blurring was slightly increased when the edge was positioned at a height of 40mm above the table compared to that measured at the table surface. In HR mode, there was surprisingly little difference between the blurring in the direction of tube motion, MTF(v), and that in the orthogonal direction when measured at the table surface. This may be due to image processing and/or sampling differences between ST and HR modes, which have different pixel sizes in projections. However, when the edge was raised to 40mm above the table, tube movement decreased MTF(v) relative to MTF(u), especially in HR mode in the direction of tube motion. The tomosynthesis projection MTF and noise for the AMULET Innovality are explored in a paper by Mackenzie *et al*.[11] This showed similar results to those in this evaluation.

4.6 Pre-processing of images

The projection images from this system have a logarithmic relationship between pixel value and dose at the detector. For the evaluation, Fujifilm also linearized the acquired images before reconstructing them to tomosynthesis planes. The results of the CDMAM measurements showed no detectable difference, and there was a 5% difference in the z-resolution between the images. It is important to use consistent methods throughout QC of a system. Overall, it would be better to use the standard logarithmic relationship to be consistent with pre-processing that will be used for clinical images.

5. Conclusions

The technical performance of the Fujifilm AMULET Innovality digital breast tomosynthesis system, in both ST and HR tomosynthesis modes was found to be satisfactory, although image quality standards have not yet been established for digital breast tomosynthesis systems. The results show a better z-resolution in HR mode than in ST mode.

In tomosynthesis mode, the MGD to the standard breast was found to be within the remedial dose levels, except at the H dose setting in HR mode. MGDs to an equivalent 53mm breast in ST and HR modes (N dose level) were 1.49mGy and 2.30mGy respectively. In H dose mode these were 1.79mGy and 2.86mGy respectively. The remedial level is 2.5mGy. It is suggested that the use of doses in tomosynthesis mode in excess of current remedial levels would need justification.

The MGDs in 2D mode were within 10% of those reported previously.[7] The measured CNRs in 2D mode were within 5% of those reported previously.[7] In 2D mode at the H dose level, recommended for NHSBSP use, the MGD to the standard breast (53mm thick) was 1.35mGy, compared to the 2.5mGy remedial level for 2D mammography.

References

1. Workman A, Castellano I, Kulama E et al. Commissioning and Routine Testing of Full Field Digital Mammography Systems (NHSBSP Equipment Report 0604 Version 3). Sheffield: NHS Cancer Screening Programmes, 2009

2. Burch A, Loader R, Rowberry B et al. Routine quality control tests for breast tomosynthesis (physicists) (NHSBSP Equipment Report 1407). London: Public Health England, 2015

3. van Engen R, Young KC, Bosmans H et al. The European protocol for the quality control of the physical and technical aspects of mammography screening. In: European Guidelines for Quality Assurance in Breast Cancer Screening and Diagnosis, 4th Edition. Luxembourg: European Commission, 2006

4. van Engen R, Bosmans H, Dance D et al. Digital mammography update: European protocol for the quality control of the physical and technical aspects of mammography screening. In: European guidelines for quality assurance in breast cancer screening and diagnosis, Fourth edition – Supplements. Luxembourg: European Commission, 2013

5. van Engen RE, Bosmans H, Bouwman RW et al. Protocol for the Quality Control of the Physical and Technical Aspects of Digital Breast Tomosynthesis Systems. Version 1.01. www.euref.org 2016

6. Moore AC, Dance DR, Evans DS et al. *The Commissioning and Routine Testing of Mammographic X-ray Systems.* York: Institute of Physics and Engineering in Medicine, Report 89, 2005

7. Strudley CJ, Oduko JM, Young KC. Technical evaluation of Fujifilm AMULET Innovality digital mammography system (NHSBSP Equipment Report 1601). London: Public Health England, 2016

8. Dance DR, Young KC, van Engen RE. Estimation of mean glandular dose for breast tomosynthesis: factors for use with the UK, European and IAEA breast dosimetry protocols. Physics in Medicine and Biology, 2011, 56: 453-471

9. Strudley CJ, Looney P, Young KC. Technical evaluation of Hologic Selenia Dimensions digital breast tomosynthesis system (NHSBSP Equipment Report 1307 Version 2). Sheffield: NHS Cancer Screening Programmes, 2014

10. Strudley CJ, Warren LM, Young KC. Technical evaluation of Siemens Mammomat Inspiration digital breast tomosynthesis system (NHSBSP Equipment Report 1306 Version 2). Sheffield: NHS Cancer Screening Programmes, 2015

11. Mackenzie A, Marshall NW, Hadjipanteli A et al. Characterisation of noise and sharpness of images from four digital breast tomosynthesis systems for simulation of images for virtual clinical trials. Physics in Medicine and Biology, 2017, 62: 2376-97